

Case Report

An Aortocaval Fistula Diagnosed with 1.5-T Magnetic Resonance Angiography

F. Walter,¹ A. Blum,¹ I. Quirin-Cosmidis,¹ Ph. Bauer,²
G. Pinelli,³ and J. Roland¹

¹Service d'Imagerie Guilloz and ²Service de Réanimation Médicale, CHU–Hôpital Central, Nancy, France

³Service de Chirurgie Cardiaque, CHU–Hôpital de Brabois, Nancy, France

ABSTRACT

We report a case of aortocaval fistula demonstrated with gadolinium-enhanced magnetic resonance (MR) angiography. Specific radiographic features of this rare complication, such as early and intense enhancement of the inferior vena cava, are underlined with MR imaging. The exact location of the fistula can also be assessed with this noninvasive imaging technique. Moreover, the absence of iodinated contrast media makes it particularly suited for stable patients with renal insufficiency. A complete preoperative assessment of abdominal aortic aneurysm can be performed with MR imaging.

KEY WORDS: Aneurism; Aorta; Arteriovenous fistula; Inferior vena cava; MR imaging.

INTRODUCTION

Abdominal aortocaval fistula (ACF) has been reported in less than 1% of surgical cases (1–4) and in approximately 4% of ruptured aneurysms (5). ACF always evolves toward severe fatal cardiac insufficiency with high output (4,5,6), and immediate surgical treatment is usually necessary (4,7). The diagnosis of ACF is difficult to assess because clinical features, such as expansive abdominal mass, dorsal pain, and blowing murmur, are identified in only 50% of cases (2,3,4,8). Among available noninvasive diagnostic tools, gadolinium-enhanced magnetic resonance (MR) angiography is particularly suited for these patients who often suffer from renal insufficiency resulting from an increased venous blood

pressure (1,5,8). We report a case of ACF diagnosed with gadolinium-enhanced MR angiography.

CASE REPORT

A 67-year-old man was admitted to the emergency room with predominant right ventricular failure. Medical history revealed a chronic renal insufficiency. Aortic valve replacement (Björk mechanical prosthesis) was performed in 1985. Clinical examination indicated a class II dyspnea; lower limb edema, mostly on the right side; and a painful enlarged liver with jugular reflux. The patient was placed after 2 days under dialysis because of aggravated renal insufficiency. Cardiac ultrasound indi-

Received July 6, 1999; Accepted April 5, 2000

Address reprint requests to A. Blum.

cated an ejection fraction of 73% and type III mitral insufficiency with proper functioning of the prosthetic aortic valve. Lower limb venous Doppler showed no sign of thrombophlebitis. On auscultation, continuous abdominal bruit was heard. A Doppler ultrasound (Toshiba, Sonolayer, SSA-270A) was subsequently performed depicting an aortic abdominal aneurysm measuring 75 mm in diameter and an arterial modulation in the inferior vena cava (IVC).

To further evaluate the aneurysm, MR angiography (Signa 1.5 T, GEMS) was performed using a T1-weighted three-dimensional spoiled GRASS (SPGR) sequence in the coronal plane (slice thickness 4 mm; TR 24 msec; TE 7 msec; $\alpha = 40^\circ$; acquisition time 3 min, 20 sec; field of view 48×48 cm; matrix 256×256 ; 1 Nex; bandwidth 16 kHz; torso array coil) with a 40-ml gadolinium intravenous injection as described by Prince (9). The bolus was injected at a constant rate for 3 min, 5 sec after the beginning of the sequence. No bolus tracking was available at the time of the examination in our institution.

The patient was instructed to breathe slowly during acquisition time. A prominent enhancement of the IVC was outlined with the same intensity as that of the aorta.

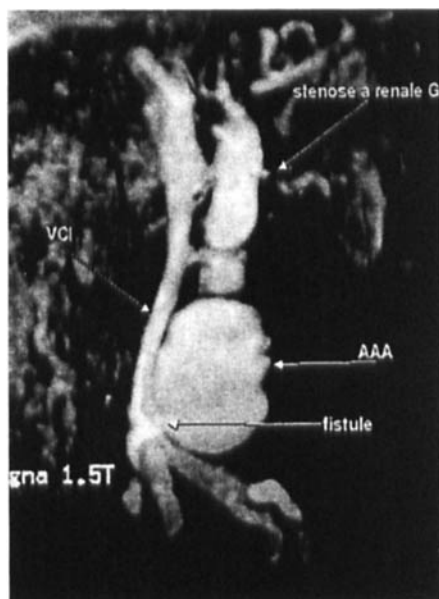


Figure 1. Coronal MIP reconstruction from three-dimensional SPGR sequence after gadolinium injection. The aneurysm (AAA) and the inferior renal portion of the inferior vena cava (VCI) intense enhancement are visible. Note a flow near the location of the fistula (arrow). A tight left renal artery stenosis is plainly visible (arrow).

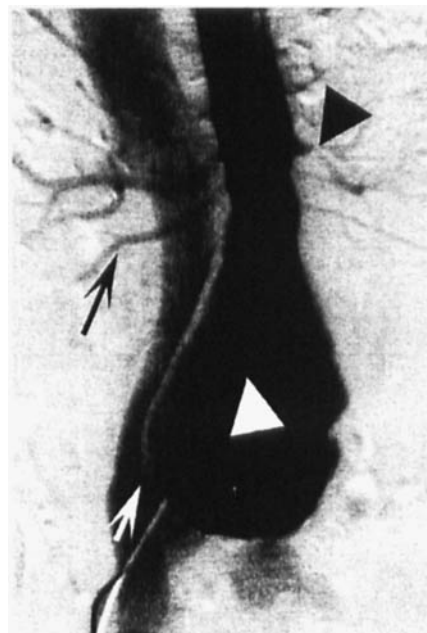


Figure 2. Digital arteriography. The aneurysm (white arrowhead) and the early enhancement of the IVC (white arrow) are highlighted. The fistula is partially visible. A narrow left renal artery stenosis (black arrowhead) and a right polar renal artery (black arrow) are confirmed.

In addition, a fistula and a flow artefact were identified above the bifurcation (Fig. 1). Then, a T1-weighted two-dimensional fast multiplanar SPGR sequence was performed in axial, coronal, and sagittal planes (TR 90 msec, TE 1.8 msec, $\alpha = 60^\circ$, slice thickness 7 mm). The fistula located on the medial rim of the aneurysm just above the bifurcation was more visible on two-dimensional axial slices or on maximum intensity projection (MIP) axial reconstruction originating from the three-dimensional sequence. A digital arteriography (Angiostar, Siemens) with right femoral artery catheterization (5 F straight catheter, 70 ml at 12 ml/sec of Visipaque 320*, Nycomed Amersham) was subsequently performed by request of the vascular surgeon, confirming a massive contrast media leakage into the IVC (Fig. 2). Fistula repair and abdominal aortic replacement were then performed, revealing a 5-cm-long fistula through an inflamed aneurysm wall. Unfortunately, the patient died several weeks after surgery because of multiorgan failure.

DISCUSSION

Spontaneous occurrence of an ACF leads to high output cardiac insufficiency resistant to medical treatment

(5). In acute forms, sudden signs of ruptured aneurysm require emergency surgical treatment. In chronic forms, however, clinical data are variable and often atypical (3,7,10). In this situation, a reliable imaging method is necessary to locate the fistula. In fact, overlooking such a fistula during surgery could result in a massive hemorrhage or pulmonary embolism originating from the wall thrombus via the fistula (5). Fistulas may originate from a progressive erosion of the wall of the IVC. The fistula is most often located at the medial site of the aneurysm just above the bifurcation, the highest pressure point (6,7).

Digital arteriography is the technique of choice. However, this invasive method necessitates injection of iodinated contrast media and is expensive and time consuming (about 45 min). In comparison, MR angiography took 25 min for this patient. Doppler imaging can outline turbulence of the IVC and iliac veins. It can also delineate the arterial flux in the IVC and perivascular artifacts in color Doppler imaging but rarely depicts the fistula itself (5). Physical conditions such as excess weight and abdominal gases can affect the final results, as well as operator experience. Helical computed tomography (CT) with the use of multiplanar and MIP reconstructions can delineate early and intense enhancement of the superior renal portion of the IVC (normally occurring around 15 sec after peak aortic enhancement) and of its inferior renal portion (normally occurring around 60 sec after peak aortic enhancement) (2,5,8,11).

Some authors report difficulties in assessing the location of the fistula using CT (1,5). Others underline the fact that normal CT findings do not totally rule out the diagnosis of ACF. In fact, intense enhancement of the subrenal IVC is fleeting and can be missed if injection and acquisition parameters are not optimal (2,11). Moreover, in patients suffering from renal insufficiency, CT with iodinated contrast media is not recommended.

To our knowledge, very few cases of ACF have been reported using MR imaging (1,12,13). In only one case (13), gadolinium injection was used to outline a fistula between the right renal artery and the IVC. In our patient's case, MR imaging showed a high enhancement of the inferior renal portion of the IVC concomitant to the aorta. Prince (9) reported that the ratio between the aortic signal and the IVC was 3.8 for a gadolinium-enhanced, three-dimensional, SPGR acquisition of 3 min, 18 sec. In our study, the ratio was 1.08. We observed that MIP reconstruction in axial plane with three-dimensional SPGR sequence and delayed axial slices with two-dimensional fast multiplanar SPGR sequence best depicted the site of the fistula above the aortic bifurcation. It must be

underlined that this relatively long sequence was appropriate to diagnose such a large fistula but may not yield such good results in less severe lesions. In fact, a faster three-dimensional gradient echo sequence (around 30 sec), as described by Holland et al. (14) with shorter TR and TE or an extrastatic gradient echo sequence (about 15 sec), may be more accurate in such cases.

Indeed, apnea acquisition allows a more precise analysis of vascular structures by diminishing kinetic artifacts (15). In our case study, digital angiography was requested by the surgical team as the standard preoperative examination. However, in our opinion, MR angiography would have been sufficient to establish an accurate diagnosis because catheter angiography did not bring any additional information. Moreover, this technique is rapid, noninvasive, and does not induce any nephrotoxicity. Consequently, when an ACF is suspected, we recommend that a three-dimensional fast gradient echo sequence in coronal plane without injection is performed to verify correct positioning of the acquisition volume. The same sequence is repeated with bolus injection during the acquisition time. Bolus tracking is advised to optimize vessel enhancement in MR angiographic images. With short time sequences, the acquisition can be repeated twice or three times for selection of the best contrast enhancement (16). MIP or VRT reconstructions may be obtained from these data. Axial and sagittal two-dimensional fast multiplanar SPGR are then performed as a final evaluation to determine anatomic variances and/or vascular wall abnormalities.

In conclusion, gadolinium-enhanced MR angiography is a noninvasive fast imaging method that allows an accurate diagnosis of ACF and is particularly suited for patients suffering from renal insufficiency.

ACKNOWLEDGMENT

We thank Professor N. Danchin, M.D., for reviewing this article and Ms. J. Zevnick for her helpful advice in the writing of the article.

REFERENCES

1. Schott EE III, Fitzgerald SW, McCarthy WJ, Nemcek AA and Sonin AH. Case report: aorto-caval fistula. Diagnosis with MR angiography. *AJR Am J Roentgenol*, 1997; 169: 59-61.
2. Clements R, Fitzgerald E and Thorpe A. Diagnosis of spontaneous aorto-caval fistula by computed tomography. *Br J Radiol*, 1986; 59:403-404.

3. Weinbaum FI, Riles TS and Imparato AM. Asymptomatic vena caval fistulization complicating abdominal aortic aneurysm. *Surgery*, 1984; 1:126–128.
4. Doty DB, Wright CB, Lamberth WC, Spoto G III, Garrett WV and Cram AE. Aorto-caval fistula associated with aneurysm of the abdominal aorta: current management using autotransfusion techniques. *Surgery*, 1978; 24: 250–252.
5. McWilliams RG, Lindsay KA and Chalmers AG. Case report: the demonstration of aorto-caval fistula by helical computed tomography. *Br J Radiol*, 1995; 68:653–656.
6. Cohen LJ, Sukov RJ, Boswell W and Ashor G. Spontaneous aorto-caval fistula. *Radiology*, 1981; 138:357–359.
7. Baker WH. Fistules aorto-caves compliquant les anévrysmes de l'aorte. In: Kieffer E, ed. Les anévrysmes de l'aorte abdominale sous-rénale. AERCIV, ed. Paris, 1990: 401–404.
8. Koslin DB, Kenney PJ, Stanley RJ and Vzn Dyke JA. Case report. Aorto-caval fistula: CT appearance with angiographic correlation. *J Comput Assist Tomogr*, 1987; 11:348–350.
9. Prince MR. Gadolinium-enhanced MR aortography. *Radiology*, 1994; 191:155–164.
10. Goodman C, Keenan RA and Logie JRC. Aorto-caval fistula. *Br J Surg*, 1984; 1:81.
11. Guth S, Clouet PL, Zöllner G, Rimmelin A, Dietemann JL and Charfe N. Fistule aorto-cave. Diagnostic par scannographie spiralee avec reconstruction 2D et 3D. *J Radiol*, 1997; 78:1159–1161.
12. Lupetin AR, Dash N and Contractor FM. MRI diagnosis of aorto-caval fistula secondary to ruptured infrarenal aortic aneurysm. *Cardiovasc Intervent Radiol*, 1987; 10:24–27.
13. Douek PC, Revel D, Chazel S, Falise B, Villard J and Amiel M. Fast MR angiography of the aorto-iliac arteries and arteries of the lower extremity: value of bolus-enhanced, whole volume subtraction technique. *AJR Am J Roentgenol*, 1995; 165:431–437.
14. Holland GA, Dougherty L, Carpenter JP, Golden MA, Gilfeather M, Slossman F, Schnall MD and Axel L. Breath-hold ultrafast three-dimensional gadolinium enhanced MR angiography of the aorta, the renal and other visceral abdominal arteries. *AJR Am J Roentgenol*, 1996; 166:971–981.
15. Prince MR, Narasimham DL, Sanley JC, Chenevert TL and Williams DM. Breath-hold gadolinium-enhanced MR angiography of the abdominal aorta and its major branches. *Radiology*, 1995; 197:785–792.
16. Walter F, Henrot P, Blum A, Hirsch JJ, Beot S, Guillemin F, Boccaccini H and Regent D. Valeur comparative de l'angio-IRM, du scanner hélicoïdal et de l'angiographie numérisée dans le bilan pré-opératoire des anévrysmes de l'aorte abdominale. *J Radiol*, 1998; 79:529–539.